Removal of acid dye (violet 54) and adsorption kinetics model of using musa spp. waste: A low-cost natural sorbent material

G. Vijaya Kumar*, P. Ramalingam*, Min Jung Kim**, Chang Kyoo Yoo**,†, and M. Dharmendira Kumar*,†

*Department of Chemical Engineering, A. C. Tech., Anna University, Chennai-600025, India
**Center for Environmental Studies/Green Energy Center, Department of Environmental Science and Engineering,
Kyung Hee University, Gyeonggi-do 446-701, Korea

Abstract−Experimental studies and biosorption kinetics of an intraparticle diffusion model for acid dye removal using a musa spp. waste sorbent were carried out to find the removal effects and dynamics of various operating parameters, such as initial dye concentration, sorbent dosage, pH and temperature. Experimental data were modeled with kinetic models and two biosorption isotherms of intraparticle diffusion models as well as the physiochemical data of sorbents characterized by SEM and FT-IR. Kinetic studies showed that the sorption process follows second-order rate kinetics with an average rate constant of 0.0018675 (g/mg·min). Thermodynamic parameters such as entropy of biosorption (ΔS^0), enthalpy of biosorption (ΔH^0) and Gibbs free energy of biosorption (ΔG^0) were obtained and analyzed. Sorbent, musa spp. waste (banana peel) was characterized by FTIR and SEM. The results showed that musa spp. waste can be considered as potential sorbent for the sorption of acid violet 54 from dilute aqueous solution.

Key words: AV 54, Biosorption, Kinetics, Intra Particle Diffusion Model, Isotherm Kinetics, Musa Spp.

INTRODUCTION

The dye effluent generated from textile industries, cosmetics, paper and food coloring industries contains dyestuffs which are one of the pollution sources. The entry of this effluent into river or any other surface water stream affects the biological activity of that system. Dyes can cause allergic dermatitis, skin irritation, cancer and mutation [1]. At present, it is estimated that more than 100,000 of commercially available over $7*10^5$ tonnes of dyestuff are produced annually [2,3]. Most of dye wastewaters are difficult to biodegrade by a microorganism due to their complex aromatic molecular structure and synthetic origin [4]. These dyes may drastically affect the photosynthetic phenomenon in aquatic life due to reduced light penetration [5,6]. Among the various kinds of dyes, available water-soluble and brightly colored acid and reactive dyes are the most problematic wastewater since they tend to pass through conventional decolorization systems unaffected [7-9].

As a result, the removal of color from waste water effluents has become environmentally important. The treatment methods for dye removal including coagulation, chemical oxidation, photo catalysis, electrochemical and biosorption techniques had been examined. Among the above-mentioned methods, biosorption is considered to be relatively superior to other techniques because of low cost, simplicity of design, ease of operation and ability to treat dyes in more concentrated form [10,11]. For the biosorption process, the well known and popular sorbent-activated carbon has been widely used. The use of activated carbon is limited due to its high cost [12,13]. Regeneration of activated carbon by refractory technique results in a 10-15% loss of sorbent and its uptake capacity. Therefore, there

is a growing interest to find low-cost, easily available materials for the biosorption of dye colors [14]. These materials include orange peel [15], rise husk [16,17], coffee husk [18], soy meal hull [19], cone biomass [20], coconut husk [21] etc. In this study banana peel is used as a sorbent.

The botanical name of banana peel is musa spp. waste. The residual component of the musa spp. waste contains holocellulose and lignin corresponding to 33 and 8.67% of the dry weight of the component, respectively [22]. In general, this musa spp. waste is disposed into landfills and rivers where it affects aquatic life. So the reuse of the musa spp. waste will be beneficial. The musa spp. waste is used as a precursor for the preparation of polyacrylamide grafted musa spp. waste having -COOH group for the removal of Co (II) from aqueous solutions [23]. In this study, the biosorption potential of musa spp. waste for the sorption of AV 54 was examined. A musa spp. waste sorbent is studied to remove acid dyes and find the removal effects of various operating parameters.

This paper is organized as follows. Section 2 provides the materials and methods which briefly explain the sorbent of Musa spp. waste and experimental methods. Section 3 shows the removal effects of various operating parameters, such as initial dye concentration, sorbent dosage, pH and temperature. Here, experimental data were modeled with kinetic models and two biosorption isotherms of intra particle diffusion models as well as the physiochemical data of sorbents characterized by SEM and FT-IR. Finally, conclusions are drawn in Section 4.
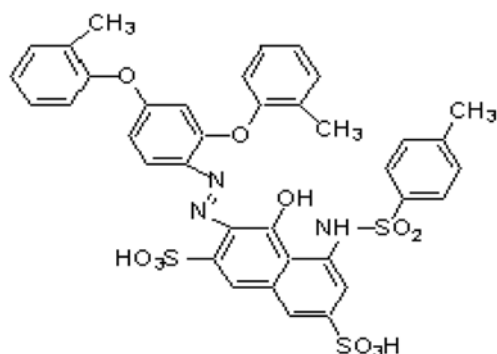
MATERIALS AND METHODS

1. Sorbate

The dye Acid Violet 54 was obtained from sd-fine chemicals, India, which was of analytical reagent grade. Stock solution was

†To whom correspondence should be addressed.
E-mail: mdkumar@annauniv.edu, ckyoo@khu.ac.kr

Acid violet 54

Scheme 1. Chemical structure of AV 54.

prepared by dissolving accurately weighed dye in double distilled water. Experimental solutions of the desired concentrations were obtained by diluting the stock solution using distilled water. The maximum wavelength of this dye is 540 nm. The structure of AV 54 is shown in Scheme 1.

2. Sorbent

The sorbent used in the study, musa spp. waste, was collected from farmland at Tiruchirappalli in India. The musa spp. waste was washed with distilled water in order to remove the surface adhered particles and impurities. Then it was sliced and dried in a hot air oven at 60 °C for 48 hours. The dried musa spp. waste was crushed and sieved in 60 mesh ASTM standard sieve to obtain a particle size 0.25 mm. It was stored in an air-tight container for further usage. No other chemical or physical treatments were used prior to the biosorption studies.

3. Experimental Methods

The batch sorption experiments were carried out in 250-mL conical flasks which contained 0.5 g of the sorbent and 100 mL of the AV 54 solutions (50-200 mg/L) operating at 150 rpm and at room temperature for 4 h and 30 min to achieve equilibrium. The pH of all solutions in contact with sorbent was found to be in the range 6.5 to 7. The concentration of the AV 54 in the solution after equilibrium sorption was measured by a double beam UV-vis spectrophotometer (Shimadzu, Model UV 1601, Japan) at 540 nm. The amount of sorption at equilibrium, q_e (mg/g), was calculated by

$$q_e = \frac{(C_0 - C_e)V}{W} \tag{1}$$

where C_0 and C_e (mg/L) are the liquid-phase concentrations of dye at initial and equilibrium, respectively. V is the volume of the solution (L) and W is the mass of sorbent used (g).

The effect of sorbent dosage was determined by adding a different amount of sorbent (0.1, 0.2, 0.3, 0.4, 0.5 and 0.6 g) to the 100 mL of dye solution and the system was kept in a shaker for the equilibrium time of 4 hours and 30 mins at 150 rpm and at 30 °C temperature. To study the effect of solution pH, 0.50 g of sorbent was added to 100 mL of 50 mg/L dye solution at 30 °C temperature (27 °C). The experiments were carried out from pH 2 to 12. The conical flasks were kept in a shaker at 150 rpm and at 30 °C temperature for 4 hours and 30 min. The concentration of the AV 54 in the solution after equilibrium sorption was measured as above. Then the effect of tem-

perature was studied for 30, 40 and 50 °C. Kinetic studies of biosorption were also done at various concentrations of the AV 54, where the extent of biosorption was investigated as a function of time. The amount of biosorption at time t, q_t (mg/g), was calculated by

$$q_t = \frac{(C_0 - C_t)V}{W} \tag{2}$$

where C_t (mg/L) is the liquid-phase concentrations of dye at any time and C_0 (mg/L) is the initial concentration of dye solution.

RESULTS AND DISCUSSION

1. Effect of Initial Dye Concentration

To investigate the effect of initial dye concentration on equilibrium uptake capacity of musa spp. waste, batch sorption experiments were carried out for different initial concentrations of AV 54 ranging from 50 mg/L to 200 mg/L at 30 °C temperature.

The variation in the equilibrium uptake capacity of musa spp. waste with contact time given different initial concentrations ranging from 50 to 200 mg/L is shown in Fig. 1. The sorption of dye in the first 60 minutes was rapid and after that sorption rate decreased gradually. The sorption rate reached equilibrium at 4 h and 30 minutes for the initial concentration of 50 mg/L to 200 mg/L. The equilibrium uptake of musa spp. waste was increased from 8.57 mg/g to 26.03 mg/g when the concentration of dye solution was increased from 50 mg/L to 200 mg/L. It is well known that the rate of exchange sorption is controlled by diffusion through a hydrostatic boundary layer, called film diffusion control or through the pores of the region matrix called particle, diffusion control. The rate of exchange sorption is mainly controlled by film diffusion under the conditions of small resin particle, dilute solution and mild stirring and vice-versa in case of pore or particle diffusion. More practically, rate of exchange sorption can be controlled by both processes [24]. Similar results were obtained in the studies of biosorption of AV 54 by various sorbents such as bagasse charcoal, brick kiln ash, cement kiln ash, cow dung charcoal, groundnut shell charcoal, used tea leaves charcoal and wheat straw charcoal was studied [25].

2. Effect of Sorbent Dosage

The effect of sorbent dosage on equilibrium uptake capacity of
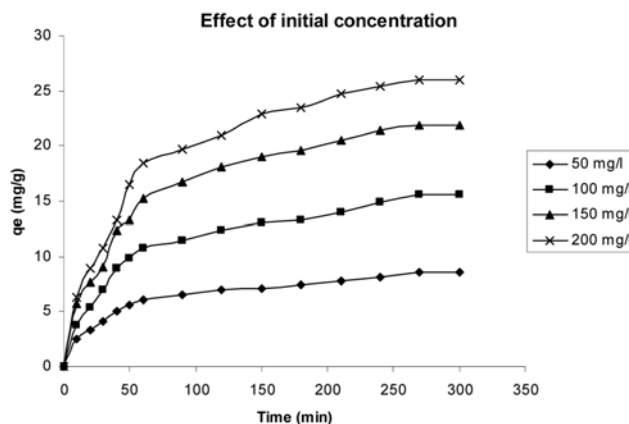
Fig. 1. Effect of initial dye concentration on the sorption of AV 54 on musa spp. waste (C_0=50 mg/L, temperature 30 °C, stirring rate 150 rpm and W=0.5 g).
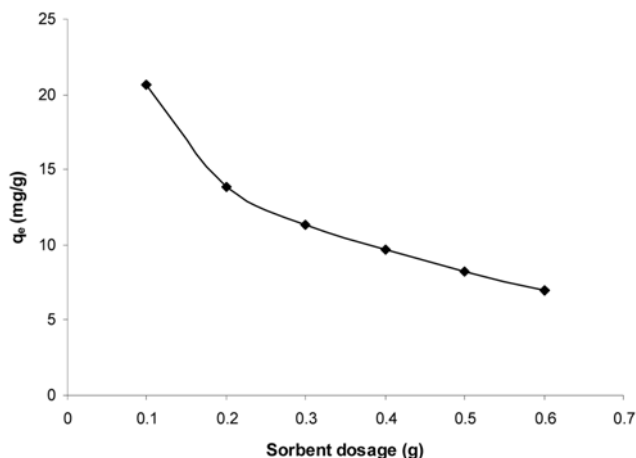
Fig. 2. Effect of Sorbent dosage on the sorption of AV 54 on musa spp. waste (C_0=50 mg/L, temperature 30 °C, stirring rate 150 rpm).

musa spp. waste is shown in Fig. 2. From Fig. 2, it was observed that when the sorbent dosage was increased from 1 g/L to 6 g/L the equilibrium uptake capacity decreased from 20.63 mg/g to 7.01 mg/g. The percentage removal of AV 54 increased from 42.08% to 85.20% with an increase in sorbent dosage from 1 g/L to 6 g/L. The resulting effect can be easily explained by an increase in surface area (more availability of active sorption sites) with the increase in sorbent mass. The amount of dye adsorbed per unit mass of sorbent decreased with increasing sorbent mass, due to the reduction in effective surface area [26,27].

3. Effect of pH

The effect of initial pH on sorption of AV 54 by musa spp. waste was studied at 50 mg/L AV 54 initial concentration at 30 °C (Fig. 3). From this figure, the maximum sorption of AV 54 was obtained at pH 2. The maximum sorption capacity for AV 54 onto musa spp. waste biosorption could be largely related to a significant electrostatic attraction existing between the surfaces of musa spp. waste and AV 54. The number of negatively charged sites increases while
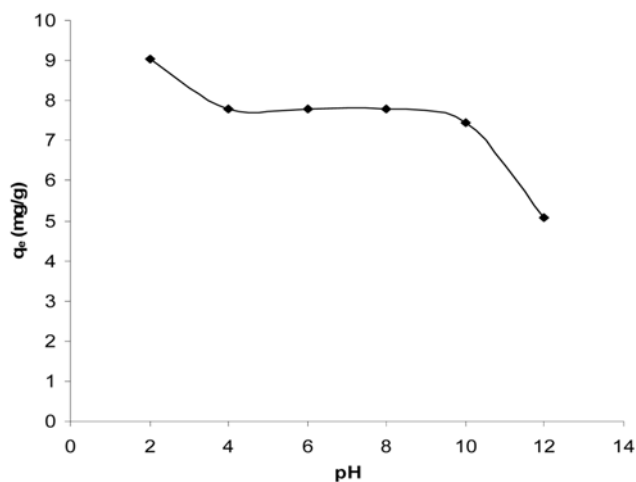

Fig. 3. Effect of the solution pH on the sorption of AV 54 on musa spp. waste (C_0=50 mg/L, temperature 30 °C, stirring rate 150 rpm and W=0.5 g).
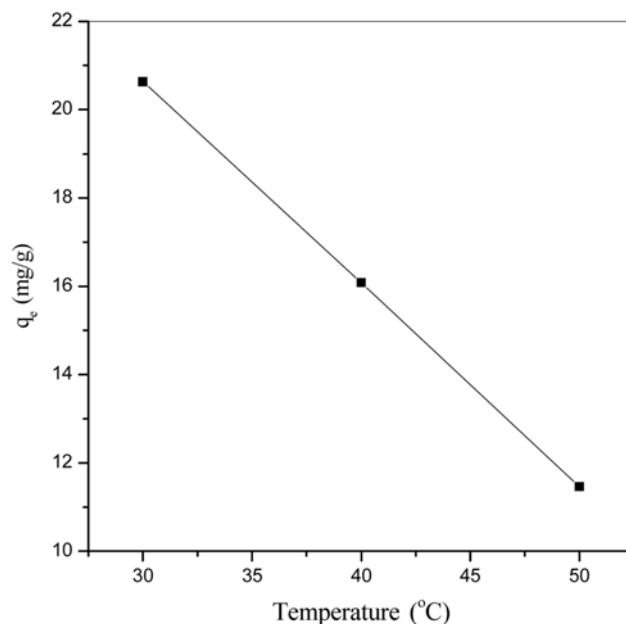

Fig. 4. Effect of temperature on the sorption of AV 54 on musa spp. waste (C_0=50 mg/L, temperature 30 °C-50 °C, stirring rate 150 rpm and W=0.5 g).

positively charged sites decrease on the sorbent surface as the solution pH increases and it remains nearly constant between pH 4 and 10. For pH 12, there is a sudden decrease in the amount of the biosorption due to competition between the excess hydroxyl ions and the negatively charged dye ions for the biosorption sites.

4. Effect of Temperature

The effect of temperature on equilibrium uptake capacity of musa spp. waste was studied at 30, 40, and 50 °C. The results in Fig. 4 show that the equilibrium uptake capacity was decreased from 20.63 mg/g sorbent to 11.46 mg/g sorbent as temperature increased from 30 to 50 °C for the dye concentration of 50 mg/L. The decrease in the sorption capacity shows that it can be a kinetically controlled process. Therefore, the sorption of AV 54 onto musa spp. waste was controlled by exothermic process. The thermodynamic parameters are considered to be the actual indicators for the application of a process. The free energy change (ΔG^0), enthalpy change (ΔH^0) and entropy change (ΔS^0) were calculated from the variation of the thermodynamic equilibrium constant K with temperature. The values of K and other thermodynamic parameters for the adsorption process were calculated by the reported methods [28] and the values of ΔH^0, ΔG^0 and ΔS^0 are shown in Table 1.

The Gibbs free energy was evaluated as

$$\Delta G^0 = -RT \ln K \tag{3}$$

where ΔG^0 is the standard Gibbs free energy change of biosorption

Table 1. Thermodynamic parameters for biosorption of AV 54 onto musa spp. waste

ΔG^0 (KJ/mol)			ΔH^0	ΔS^0
30 °C	40 °C	50 °C	(KJ/mol)	(KJ/mol·K)
−4103.32	−2297.21	−1394.83	−44.986	−0.13542

(J), R is the universal gas constant (8.314 J/(mol·K)), T is the absolute temperature (K) and K is the equilibrium constant. Enthalpy of biosorption (ΔH^0) and entropy of biosorption (ΔS^0) values can be obtained as

$$\Delta G^0 = \Delta H^0 - T\Delta S^0 \tag{4}$$

The Gibbs free energy of biosorption (ΔG^0) for the system of AV 54/musa spp. waste is -4103.32, -2297.21 and -1394.83 KJ/mol at 30, 40 and 50 °C, respectively. The enthalpy of biosorption (ΔH^0) is -44.986 KJ/mol and the entropy of biosorption (ΔS^0) is -0.1354 KJ/mol·k at the temperature 30 °C. The negative ΔH^0 indicates that the sorption is exothermic in nature. The negative ΔS^0 reveals that a more ordered arrangement of AV 54 is shaped on the adsorbent surface. The negative ΔG^0 implies a favorable and spontaneous sorption process, and it is independent on the adsorption capacity.

5. Sorption Isotherms

The biosorption data were analyzed using sorption isotherm models, namely Langmuir and Freundlich. The Langmuir biosorption model [29] is based on the assumption that maximum biosorption corresponds to a saturated monolayer of solute molecules on the sorbent surface. The expression of the Langmuir model is given by the following equation

$$q_e = \frac{Q_0 b C_e}{1 + b C_e} \tag{5}$$

where q_e (mg/g) and C_e (mg/L) are the amount of adsorbed dye per unit mass of sorbent and unadsorbed dye concentration in solution at equilibrium, respectively. Q_0 is the maximum amount of the adsorbed dye per unit mass of sorbent to form a complete monolayer on the surface bound at high C_e (mg/g), and b (L/mg) is a constant related to the affinity of the binding sites. The linear form of the Langmuir equation is written as follows:

$$C_e/q_e = 1/Q_0 b + C_e/Q_0 \tag{6}$$

According to Eq. (7), when the adsorption is assumed to be followed by the Langmuir equation, a plot of (C_e/q_e) versus C_e should be a straight line with a slope of 1/Q_0 and intercept $1/Q_0 b$. The essential characteristics of the Langmuir isotherm can be expressed in terms of a dimensionless constant separation factor R_L that is given by the following equation [30]:

$$R_L = \frac{1}{1 + bQ_0} \tag{7}$$

where C_0 (mg/L), is the highest initial concentration of adsorbate and b is Langmuir constant. The parameter R_L indicates the nature of the shape of the isotherm accordingly, where $R_L > 1$ means an unfavorable biosorption, $0 < R_L < 1$ means a favorable biosorption, $R_L = 0$ means an irreversible biosorption, and $R_L = 1$ means a linear biosorption.

The Freundlich model [31] assumes heterogeneous biosorption due to the diversity of biosorption sites. The Freundlich equation is expressed as

$$q_e = K_F C_e^{1/n} \tag{8}$$

where K_F (mg/g) is roughly an indicator of the biosorption capacity and 1/n (L/mg) is the biosorption intensity. The magnitude of the exponent, 1/n, gives an indication of the favorability of bio-

sorption. Values of n>1 represent favorable biosorption conditions [32,33]. Eq. (9) can be written in the logarithmic form as

$$\ln q_e = \ln K_F + (1/n)\ln C_e \tag{9}$$

The values of K_f and n can be obtained from the slope and intercept of the plot of log q_e against log C_e.

The Langmuir and Freundlich isotherms for the sorption of AV 54 onto musa spp. waste at 30 °C temperature are shown in Figs. 5 and 6. The Langmuir and Freundlich biosorption constants of the isotherm kinetics at 30 °C with the correlation coefficients are listed in Table 2. As seen, a very high regression correlation coefficient was shown by the Langmuir model. This indicates that the Lang-
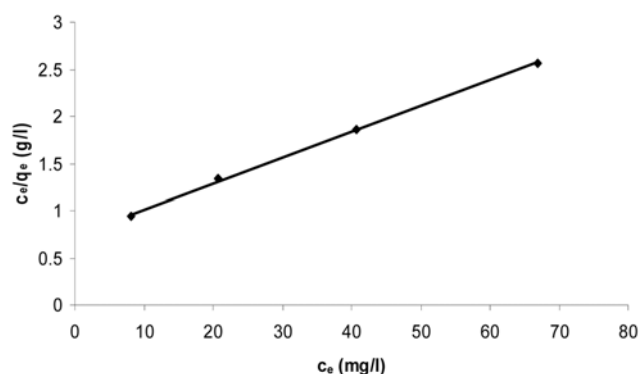

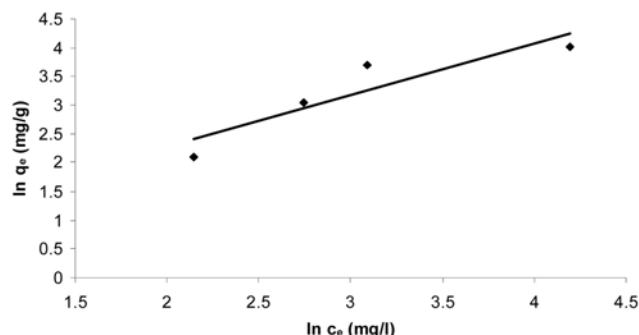Fig. 5. Langmuir isotherm for AV 54 sorption onto musa spp. waste at 30 °C temperature.

Fig. 6. Freundlich isotherm for AV 54 sorption onto musa spp. waste at 30 °C temperature.

Table 2. Langmuir and Freundlich parameters for biosorption of AV 54 onto musa spp. waste at room temperature

Isotherm	Parameters
Langmuir	
Q_0 (mg/g)	36.496
b (L/mg)	0.0369
R^2	0.9993
R_L	0.3472
Freundlich	
K_f (mg/g)	1.5708
n (L/g)	1.102
R^2	0.8334

muir model was very suitable for describing the sorption of AV 54 by musa spp. waste. The maximum capacity Q_0 determined from the Langmuir isotherm defines the total capacity of the biosorbent for the dye as 36.496 mg/g sorbent. The fact that the Langmuir isotherm fits the experimental data very well may be due to the homogeneous distribution of active sites on the surface of sorbent, since the Langmuir equation assumes that the surface is homogeneous. The values of R_L in the present investigation have been found to be 0.3472 at 30 °C, indicating that the biosorption of AV 54 on musa spp. waste is favorable. Table 2 also shows that the n value is greater than 1, which indicates a favorable biosorption.

6. Sorption Kinetics

To investigate the mechanism of the sorption of AV 54 onto musa spp. waste, the pseudo-first-order, pseudo-second-order kinetics and intra particle diffusion model were applied to the experimental data. The linear form of Lagergren's pseudo-first-order rate equation is as follows [34].

$$\log(q_e - q_t) = \log q_e - \frac{K_1}{2.303}t \tag{10}$$

A linear fit of $\log(q_e - q_t)$ versus t shows the applicability of this kinetic model. The pseudo-first-order rate constant (k_1) and q_e values were determined from the slope and intercept. The integrated linear form of pseudo-second-order equation is [35]

$$\frac{t}{q_t} = \frac{1}{k_2 q_{2e}} + \frac{1}{q_e}t \tag{11}$$

where k_2 (g/mg min) is the pseudo-second-order rate constant determined from the plot of t/q_t vs t.

The straight line plots for the pseudo-first-order reaction and pseudo-second-order reaction of the sorption of AV 54 by musa spp.
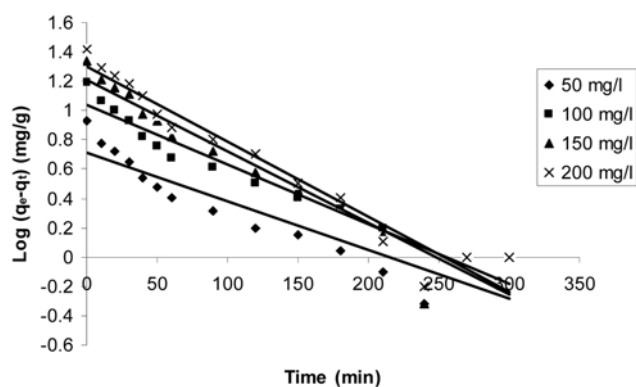
waste are shown in Fig. 7 and 8. The calculated value of k_1, k_2, q_e and their corresponding regression coefficient values (R^2) are presented in Table 3. In many cases the first-order equation of Lagergren does not fit well to the whole range of contact time and is generally applicable over the initial stage of the biosorption processes [36]. Although the correlation coefficients (R^2) for the application of the pseudo-first-order model are reasonably high in some cases, the calculated q_e is not equal to experimental q_e, suggesting the biosorption of AV 54 on of biosorption is not likely to be a pseudo-first-order for the initial concentrations examined. Table 3 shows that the coefficients for the pseudo-first-order kinetic model obtained at all the studied concentrations were low. Also, the theoretical q_e values found from the pseudo-first-order kinetic model did not give reasonable values. This suggests that this sorption system is not a first-order. The calculated q_e values agree very well with the experimental values for the case of pseudo-second-order kinetics, and a regression coefficient of above 0.98 shows that the model can be applied for the entire biosorption process.

6-1. Intraparticle Diffusion

The intraparticle diffusion model suggested by Weber and Morris [37] is tested to identify the diffusion mechanism using the following equation:

$$q_t = k_i t^{1/2} + C \tag{12}$$

where k_i is the intraparticle diffusion rate constant (mg/g min$^{1/2}$) and C (mg/g) is a constant that gives an idea about the thickness of the boundary layer, i.e., the larger the value of C the greater the boundary layer effect. If the Weber-Morris plot of qt vs $t^{1/2}$ gives a straight line, then the sorption process is controlled by intraparticle diffusion only. The coefficients values ($R^2 > 0.99$) and intraparticle diffusion constants which are obtained from the slope of Fig. 9 are listed in the Table 4. The high coefficient values suggest that the biosorption
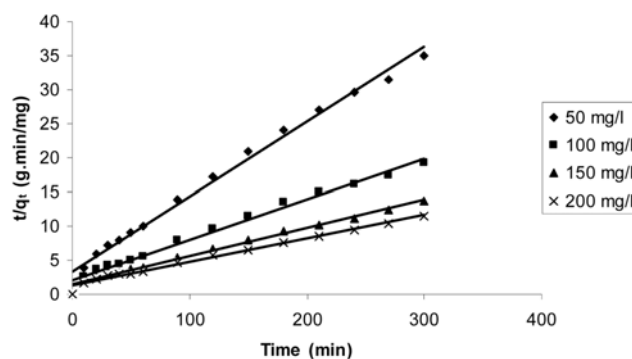

Fig. 7. Pseudo-first-order sorption kinetics of sorption of AV 54 onto musa spp. waste.

Fig. 8. Pseudo-second-order sorption kinetics of sorption of AV 54 onto musa spp. waste.

Table 3. Pseudo-first-order and pseudo-second-order rate constants for the biosorption of AV 54 onto musa spp. waste

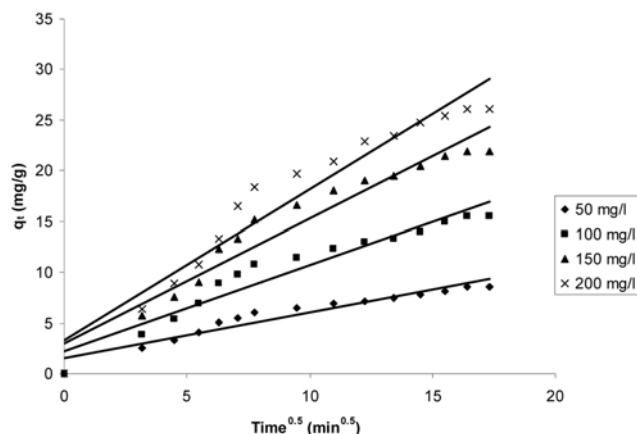| Initial conc	$Q_{e, exp}$ (mg/g)	Pseudo-first-order kinetic model			Pseudo-second-order kinetic model		
		K_1 (1/min)	$q_{e, cal}$ (mg/g)	R^2	K_2 (g/mg·min)	$q_{e, cal}$ (mg/g)	R^2
50	8.57142	0.0076	5.122	0.8386	0.00369	9.107	0.9888
100	15.5555	0.0094	10.269	0.9344	0.00171	16.835	0.9858
150	21.9047	0.0112	16.195	0.9314	0.00117	24.154	0.9874
200	26.0317	0.0117	19.943	0.9524	0.0009	28.985	0.9866

Fig. 9. Plots for evaluating intraparticle diffusion rate constant for sorption of AV 54 onto musa spp. waste.

Table 4. Intraparticle diffusion constants for différent initial AV 54 concentrations

Initial concentration (mg/L)	k_i (mg/g min$^{1/2}$)	C	$q_{e, cal}$ (mg/g)	R^2
50	0.4502	1.5267	9.324393	0.9228
100	0.8487	2.2384	16.93832	0.9332
150	1.2329	2.9815	24.33595	0.9365
200	1.4871	3.2803	29.03763	0.9368

mechanism involves an intraparticle diffusion, but the fact that the plot does not pass through the origin indicates that intraparticle diffusion was not the only rate-controlling step. Other kinetic models may control the biosorption rate.

7. SEM and FTIR of Musa Spp. Waste

The surface structure of musa spp. waste before sorption of AV 54 was analyzed by scanning electron microscope with magnification of 50 µm at 5 KV (Fig. 10). As shown in the SEM micrograph, high porous surface was found to be more on the surface of the musa spp. waste. This figure also reveals that the pores on the surface of the musa spp. waste are highly homogeneous. The pores on the sur-
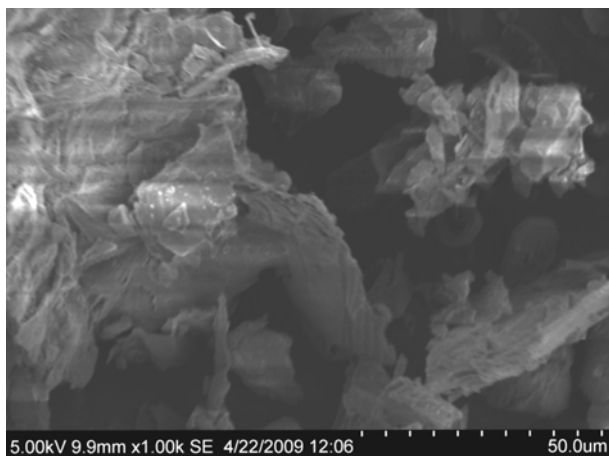

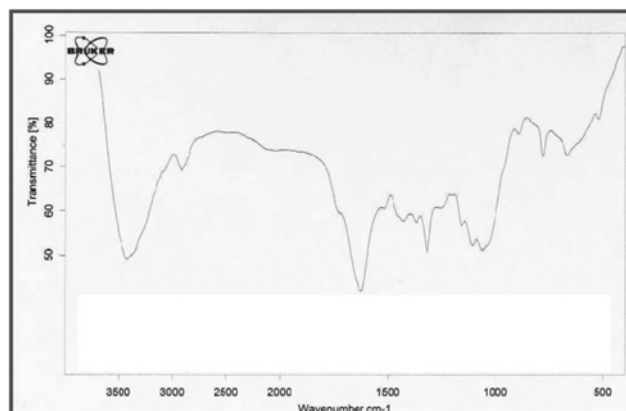**Fig. 10. Scanning electron microscope of musa spp. waste (before adsorption).**

Fig. 11. FTIR spectrum of musa spp. waste (before adsorption).

face of the musa spp. waste are an important factor for the sorption of AV 54. The FTIR spectrum of musa spp. waste was obtained to identify the functional groups in musa spp. waste (Fig. 11). The FTIR spectrum showed the following bands, which are an O-H stretch (3,500-3,400 cm^{-1}), a C-H stretch (2,900-3,000 cm^{-1}), a C=C stretch (1,700-1,600 cm^{-1}), a C-(CH$_3$)$_2$ (1,300-1,400 cm^{-1}), a C-O stretch (1,106.17 cm^{-1}), a C-O-C stretch (1,062.51 cm^{-1}), and a C-OH stretch (666.44 cm^{-1}).

CONCLUSION

Musa spp. waste is identified as an effective sorbent for the removal of AV 54 dye from aqueous solution. The sorption is highly dependent on various operating parameters such as initial dye concentration, contact time, and sorbent dosage. The percentage of biosorption decreases from about 84.1% to 66.1% as the initial dye concentration increases from 50 mg/L to 200 mg/L at the end of the equilibrium time. The percentage biosorption increases from 42.1% to 85.2% as the sorbent dosage increases from 0.1 g to 0.6 g for 50 mg/L. The dye uptake was maximum at pH 2.The sorption of AV 54 onto of biosorption was controlled by exothermic process. The experimental data were best correlated by Langmuir isotherm. The sorption kinetics of AV 54 onto musa spp. waste is well described by pseudo-second-order kinetics.

NOMENCLATURE

AV 54 : acid violet 54
b   : the constant related to the affinity of the binding sites [L/mg]
C_0 : the liquid-phase concentrations of dye at initial [mg/L]
C_e : the liquid-phase concentrations of dye at equilibrium [mg/L]
$C_{ad, e}$: the equilibrium concentration of dye on the sorbent [mg/g]
C_t : the liquid-phase concentrations of dye at any time [mg/L]

G : the standard Gibbs free energy change [KJ/mol]
H : the enthalpy change [KJ/mol]
K : the apparent equilibrium constant
K_F : the Freundlich constant [mg/g]
k_2 : the pseudo-second-order rate constant [g/mg min]
k_i : the intraparticle diffusion rate constant [mg/g min$^{1/2}$]
n : dimensionless exponent of Freundlich equation
q_t : the amount of biosorption at time t [mg/g]
q_e : the amount of adsorbed dye per unit mass of sorbent [mg/g]
Q_0 : the maximum amount of the adsorbed dye per unit mass of sorbent [mg/g]
R_L : dimensionless constant separation factor
R : the universal gas constant [8.314 J/(mol·K)]
S : the entropy change [KJ/mol·K]

REFERENCES

1. P. K. Ray, *J. Sci. Ind. Res.*, **45**, 370 (1986).
2. J. W. Lee, S. P. Choi, R. Thiruvenkatachari, W. G. Shim and H. Moon, *Dyes Pigments*, **69**, 196 (2006).
3. P. Nigam, G. Armour, I. Banat, MD. Singh and R. Merchant, *Bioresour. Technol.*, **72**, 219 (2000).
4. S. Seshdari, P. L. Bishop and A. M. Agha, *Waste Manage.*, **15**, 127 (1994).
5. K. R. Ramakrishna and T. Viraraghavan, *Water Sci. Technol.*, **36**, 189 (1997).
6. V. K. Garg, R. Kumar and R. Gupta, *Dyes Pigments*, **62**, 1 (2004).
7. Z. Aksu, *Process Biochem.*, **40**, 997 (2005).
8. S. W. Won, S. B. Choi and Y. S. Yun, *Colloids Surfaces A: Phys. Eng. Aspects*, **262**, 175 (2005).
9. S. W. Won, S. B. Choi and Y. S. Yun, *Biochem. Eng. J.*, **28**, 208 (2006).
10. V. Meshko, L. Markovska, M. Mincheva and A. E. Rodrigues, *Water Res.*, **35**, 3357 (2001).
11. N. Kannan and M. M. Sundaram, *Dyes Pigments*, **51**, 25 (2001).
12. M. S. EL-Geundi, *Adsorpt. Sci. Technol.*, **15**, 777 (1997).
13. G. Annadurai, R. S. Juang and D. J. Lee, *Adv. Environ. Res.*, **6**, 191 (2002).
14. P. Waranusantigul, P. Pokethitiyook, M. Kruatrachue and E. S. Upatham, *Environ. Pollut.*, **125**, 385 (2003).
15. C. Namasivayam, N. Muniasamy, K. Gayatri, M. Rani and K. Renganathan, *Biores. Technol.*, **57**, 37 (1996).
16. R. Han, Y. Wang, W. Yu, W. Zou, J. Shi and H. Liu, *J. Hazard. Mater.*, **141**, 713 (2007).
17. T. G. Chuah, A. Jumasiah, I. Azni, S. Katayon and S. Y. Thomas Choong, *Desalination*, **175**, 305 (2005).
18. Leandro S. Oliveira, Adriana S. Franca, Thiago M. Alves and Sonia D. F. Rocha, *J. Hazard. Mater.*, **155**, 507 (2008).
19. M. Arami, N. Y. Limaee, N. M. Mahmoodi and N. S. Tabrizi, *J. Hazard. Mater.*, **B135**, 171 (2006).
20. A. T. Akar, S. Ozcan, S. Tunali and A. Ozcan, *Bioresour. Technol.*, **99**, 3057 (2008).
21. B. H. Hameed, D. K. Mahmoud and A. L. Ahmad, *J. Hazard. Mater.*, **158**, 65 (2008).
22. R. G. Medeiros, M. L. A. Soffner, J. A. Thome, A. O. G. Cacais, R. S. Estelles, B. C. Salles, H. M. Ferreira, S. A. Lucena Neto, F. G. Silva Jr. and E. X. F. Filho, *Biotechnol. Progr.*, **16**, 522 (2000).
23. I. G. Shibi and T. S. Anirudhan, *Chemosphere*, **58**, 1117 (2005).
24. S. K. Srivastava, V. K. Gupta and Dinesh Mohan, *J. Env. Modeling Assessment*, **1**, 281 (1998).
25. Sumanjit, T. P. S. Walia and R. Kaur, *J. Health Allied Scs.*, **3**, 3 (2007).
26. G. Vijayakumar, M. Dharmendirakumar, S. Renganathan, S. Sivanesan, G. Baskar and K. P. Elango, *Clean-soil Air Water*, **37**(4-5), 355 (2009).
27. B. K. Nandi, A. Goswami, A. K. Das, B. Mondal and M. K. Purkait, *Sep. Sci. Technol.*, **43**, 1382 (2008).
28. V. Vadivelan and K. Vasanthakumar, *J. Colloid Interf. Sci.*, **286**, 91 (2005).
29. I. Langmuir, *J. Am. Chem. Soc.*, **40**, 1361 (1918).
30. K. R. Hall, L. C. Eagleton, A. Acrivos and T. Vermeulen, *IEC Fundam.*, **5**, 212 (1966).
31. H. Freundlich, *J. Phys. Chem.*, **57**, 384 (1906).
32. R. E. Treybal, *Mass Transfer Operations*, 2nd Ed., McGraw Hill, New York (1968).
33. Y. S. Ho and G. McKay, *Chem. Eng. J.*, **70**, 115 (1978).
34. S. Lagergren, *Handlingar.*, **24**, 1 (1898).
35. G. McKay and Y. S. Ho, *Water Res.*, **33**, 578 (1999).
36. W. J. Weber and J. C. Morris, Proceedings of the International Conference on Water Pollution Symposium 2, Pergamon, Oxford, 231 (1962).
37. W. J. Weber and Jr. J. C. Morris, *J. Sanitary Eng. Div. Proceed. Am. Soc. Civil Eng.*, **89**, 31 (1963).